IOP PUBLISHING JOURNAL OF PHYSICS D: APPLIED PHYSICS

J. Phys. D: Appl. Phys. **40** (2007) R93–R107 doi:10.1088/0022-3727/40/5/R01

TOPICAL REVIEW

Slow light in semiconductor heterostructures

P C Ku[1], C J Chang-Hasnain[2] and S L Chuang[3]

[1] Department of Electrical Engineering and Computer Science, University of Michigan, 1301 Beal Av, Ann Arbor, MI 48109, USA
[2] Department of Electrical Engineering and Computer Science, University of California at Berkeley, Berkeley CA 94720, USA
[3] Department of Electrical and Computer Engineering, University of Illinois at Urbana-Champaign, Urbana, IL 61801, USA

E-mail: peicheng@umich.edu

Received 1 August 2006, in final form 10 January 2007
Published 16 February 2007
Online at stacks.iop.org/JPhysD/40/R93

Abstract

This paper presents an overview of slow light in semiconductor heterostructures. The focus of this paper is to provide a unified framework to summarize and compare various physical mechanisms of slow light proposed and demonstrated in the past few years. We expand and generalize the discussions on fundamental limitation of slow light and the delay–bandwidth product trade-off to include gain systems and other mechanisms such as injection locking. We derive the maximum fractional delay and compare the differences between material dispersion and waveguide dispersion based devices. The delay–bandwidth product is proportional to the square root of the device length for a material dispersion based device but has a linear relationship for a waveguide dispersion based device. Possible scenarios to overcome the delay–bandwidth product limitation are discussed. The prospects of slow light in various applications are also investigated.

(Some figures in this article are in colour only in the electronic version)

1. Introduction

Slow light, i.e. optical signal propagating at a velocity much slower than the speed of light in the vacuum, has attracted unprecedented attentions in the past few years. When an optical signal travels through a slow light device, its signal velocity slows down. If the signal distortion after passing through the device is small enough that all the information it carries can be recovered at the output, the signal velocity is equivalent to the group velocity and is given by the following formula:

$$v_g = \frac{c - \omega(\partial n/\partial\beta)}{n + \omega(\partial n/\partial\omega)}, \tag{1}$$

where n is the refractive index as a function of both the frequency ω and the propagation constant β. Slow light is scientifically interesting not only because an optical signal travelling at a bicycle speed cannot be observed in a typical material but because it also provides potential solutions to several challenging problems in various engineering applications including variable optical delay lines or optical buffers [1], low-light level nonlinear optical devices [2], optical pulse synchronization and reshaping [3], all-optical signal as well as quantum information processing, true-time delay (TTD) in a phased-array antenna (PAA) [4,5] and miniaturization of many spectroscopy systems due to the availability of a variable delay line. According to (1), a slow light device needs to exhibit either a large material dispersion (i.e. a large and positive $\partial n/\partial\omega$) or a large waveguide dispersion (i.e. a large and positive $\partial n/\partial\beta$). In the case of material dispersion, a large and positive $\partial n/\partial\omega$ corresponds to a spectral hole or a gain peak in an absorption background. From the Kramers–Krönig (KK) relation, the slow down factor S ($\equiv c/v_g$) can be expressed as the integral of the imaginary part of the dielectric constant $\mathrm{Im}\varepsilon(\omega)$ as follows [6, 7]:

$$S(\omega) = n_{bac} + \frac{1}{2\pi n_{bac}} \mathrm{PV} \int_{-\infty}^{\infty} \frac{\mathrm{Im}\varepsilon(\omega')}{(\omega' - \omega)^2} \mathrm{d}\omega', \tag{2}$$

 © 2007 IOP Publishing Ltd Printed in the UK

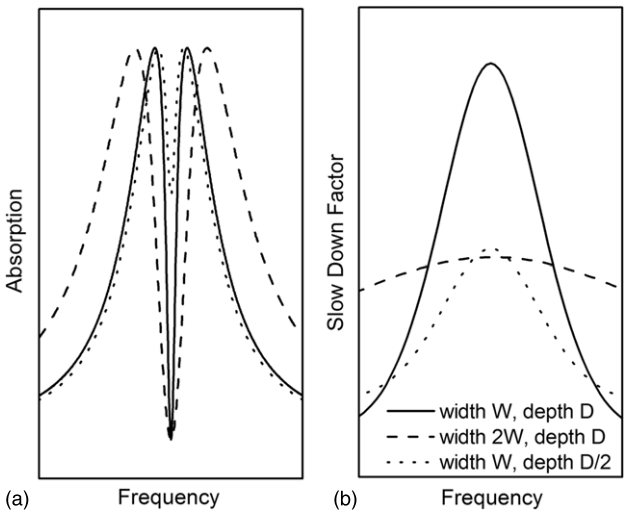

Figure 1. The narrow spectral hole (or a gain peak) in an absorption background in (*a*) creates a steep change in the refractive index and leads to slow light as shown in (*b*). Three different spectral hole widths and depths and their corresponding slow down factors are compared. The slow down factor at the centre of the spectral hole is inversely proportional to the width and is proportional to the depth of the transparency window, respectively.

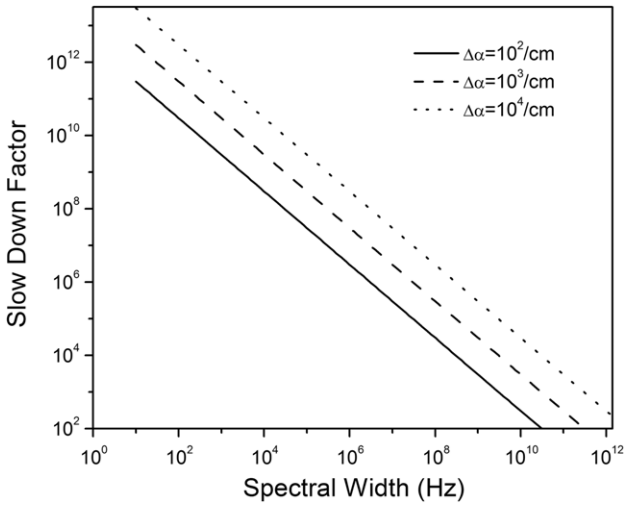

Figure 2. Slow down factor versus the width of the spectral hole (or the gain peak) for a series of different spectral hole depths ($\Delta\alpha$) in a typical semiconductor material with a refractive index of 3.6. The slow down factor is inversely proportional to the width of the spectral hole and proportional to the depth of the spectral hole.

where n_{bac} is the background refractive index of the material far away from the absorption region and PV is the principal value of the integral. The function $\mathrm{Im}\varepsilon(\omega)$ corresponds directly to the characteristics of the spectral hole. As illustrated in figure 1 and will be derived later in Section 3, the slow down factor is inversely proportional to the width of the spectral hole (or gain peak) and is also proportional to its depth. In order to achieve a large slow down factor S ($\equiv c/v_{\mathrm{g}}$), a narrow and deep transparency window is required. Figure 2 plots the maximum achievable slow down factor versus the width and the depth ($\Delta\alpha$) of the spectral hole for a typical semiconductor material. To achieve a slow down factor of 10^4, a spectral hole as narrow as a few GHz wide is necessary. This explains why slow light cannot be easily observed in nature.

The drastic change in group velocity, whether slow or fast light, has attracted the attentions of many researchers for a long time. In 1982, Chu and Wong [8] observed that an optical pulse propagating through an absorbing semiconductor material can experience a superluminal group velocity. Earlier experiments of slow light in semiconductor materials have also been reported both with material dispersion [9–11] and with waveguide dispersion [12–15]. The slow down factors reported in these experiments were, however, rather limited either due to weak modulation of grating refractive indices or due to rapid decoherence processes in semiconductors as a result of carrier–carrier and carrier–phonon interactions. These processes were not able to generate narrow enough spectral holes and therefore did not considerably slow down the group velocity of light. In 1991, Harris *et al* [16, 17] first demonstrated a narrow transparency window induced in an otherwise opaque medium. The interaction of the optical signal with a strong pump laser via a non-radiative coherent process in a three-level system cancels out the absorption of the signal beam completely. This phenomenon is called electromagnetically induced transparency (EIT) and later laid a foundation for the development of slow light. EIT demonstrated for the first time that we can explore an ultra-narrow transparency window without an excessive absorption loss. In the last one and a half decade, slow light in a variety of material systems using different physical mechanisms has been successfully demonstrated in experiments. These include slow light by EIT in Bose–Einstein condensates [18], atomic vapours [19, 20], and solid crystals [21]; slow light by coherent population oscillation (CPO) in solid crystals [22], semiconductor quantum wells (QWs) [23–26] and semiconductor quantum dots (QDs) [27,28]; slow light in gain systems including stimulated Raman or Brillouin scattering (SRS and SBS) in solid atoms [29], optical fibres [30] and silicon-on-insulator waveguides [31] as well as the optical gain of vertical cavity surface emitting lasers (VCSELs) operating in the amplifier regime [32]; slow light by exciton dephasing in semiconductor QWs [33]; slow light in semiconductor optical amplifiers (SOA) [34, 35] by four-wave mixing and CPO; slow light by optical injection locking (OIL) [36]; slow light via gratings in a photorefractive crystal [37] and slow light in photonic crystal and resonator structures [38–40]. Among them, slow light in optical fibres and semiconductor heterostructures are most suitable for practical applications. In this paper, we will focus mainly on slow light in semiconductor heterostructures. Readers who are interested in aspects of slow light in optical fibres or other material systems can refer to excellent reviews in [41–43].

Slow light in semiconductor materials can enable ultra-compact variable optical delay lines with electrical controllability. They have low power consumption and can be integrated with other electronics as well as optoelectronics devices. These are aspects difficult to achieve in other material systems including optical fibres. The development of slow light in semiconductors has been limited until the last couple of years. Earlier experiments did not have access to processes which can lead to sufficiently narrow transparency windows and hence resulted in small slow down factors. In 1990,

Table 1. Comparison of several benchmarking parameters for different slow light applications. The gauge used in the table is defined as follows. A 'moderate' total delay is defined to be ∼1 ns and 'large' means an order of magnitude larger than the moderate value. Similarly, a moderate $\delta S/S$ is defined to be ∼10%, and a moderate B to be ∼1 GHz, a moderate operating speed to be ∼100 MHz. These definitions are only for the purpose of convenience. RT stands for room temperature. Low temperature means the operating temperature needs to be lowered to the liquid nitrogen temperature or below.

	$\Delta\tau$	$\Delta S/S$	B	Operating speed	Operating temperature
Optical buffers [48, 49]	Moderate	Large	Large	Slow	RT
Pulse synchronization [50]	Small	Small	Large	Slow	RT
Phased-array antenna [51]	Small	Moderate	Moderate	Moderate	RT
All-optical signal processing [52]	Large	Large	Large	Fast	RT
Quantum information [53]	Small (in the near future)	Small	Small	Moderate	Low–RT

Wang *et al* [44] showed that a narrow transparency window can be created in semiconductor materials by the beating of two laser beams (one strong and one weak) with frequencies very close to each other. The beating generates a temporal grating followed by the carriers inside the semiconductors and induces an energy exchange between the two laser beams which leads to a narrow transparency window experienced by the weak beam. This phenomenon is called CPO and is different from EIT in that it only requires a two-level system instead of a three-level one. But the transparency window created by CPO does not suppress the absorption completely as it does in an ideal EIT system. In spite of this, slow light by CPO in QWs was demonstrated experimentally by Ku *et al* in 2003 [23]. A constant slow down factor of 32 000 over a spectral range of 2 GHz was reported. This was the first time an appreciable slow down factor was observed in semiconductor materials. Recently CPO has been reported in other types of semiconductor heterostructures such as QDs [27, 28] and the operating temperature has been improved from below 100 K to room temperature (RT) [24, 25].

Slow light is a multi-disciplinary field. It would be an insurmountable job for us trying to cover every aspect of slow light. We instead take the liberty of choosing an application oriented approach. We will focus on a few key parameters of slow light that are most relevant in applications and use those as benchmarks to compare different slow light mechanisms. We will also systematically discuss how these parameters are related to material properties in a unified theoretical framework and discuss ultimate limitations of slow light in applications. We hope in this way the readers can more easily bridge the gap between the physics behind slow light and the design trade-offs. The organization of this paper is as follows. In section 2, we first identify a few applications and define the key parameters and their respective requirements in different applications. In section 3, we will present the general principle of slow light using a unified theoretical framework and discuss limitations of slow light and possible approaches to overcome these limits. In section 4, we will review various slow light experiments in semiconductor heterostructures including CPO in QWs and QDs, slow light in SOA and OIL-VCSEL, etc. We will also discuss and compare slow light in photonic crystal and resonator structures. The paper will be concluded with a brief summary of the status quo of the slow light in applications and with discussions of several future aspects of slow light.

2. Slow light applications

Applications of slow light can be quite broad but the most basic one is a variable optical delay line. By modulating the material dispersion $\partial n/\partial\omega$, the amount of delay can be changed without physically changing the device length. The ability to change the delay without mechanically stretching or shrinking the optical path has a profound impact on the adoption of this kind of device in applications. In many occasions, a compact delay line is necessary. In a phased-array antenna as an example, hundreds of delay lines need to be packed into a small system. With a large slow down factor, a very compact variable delay line can be realized. With a slow down factor of 10^4, a slow light device of 100 μm can achieve a 3 ns delay while a piece of fibre with a length of 60 cm is required to achieve the same amount of delay!

In addition to generating a variable time delay for an optical signal, slow light also increases the efficiency of the nonlinear optical effect by increasing the total amount of time the optical signal stays in the slow light device. This effectively increases the interaction length and reduces the intensity required to achieve the same degree of efficiency for a nonlinear optical process.

The above two basic operations of a slow light device can lead to many specific applications. A few of them are identified and summarized in table 1. In the table, several benchmarking parameters including the total time delay $\Delta\tau$, the slow down factor S, the variability of the slow down factor $\Delta S/S$, the operating bandwidth B and the operating speed are defined. We distinguish the operating bandwidth from the operating speed. The latter refers to how fast we can change the slow down factor from one value to another while the former refers to the frequency range within which the slow down factor is a constant in order to avoid excessive distortion on the optical signal. As an example, for optical buffers in a packet-switched network, the slow down factor as a function of the signal modulation frequency needs to be a constant over the entire signal spectral range. But if the slow light device is to generate a variable delay for a single optical pulse, this stringent requirement can be greatly relaxed because an isolated optical pulse is more immune to distortion such as pulse widening compared with a pseudo-random pulse train in a telecommunication network [45, 46]. On the other hand, a digitally modulated signal has more tolerance in distortion

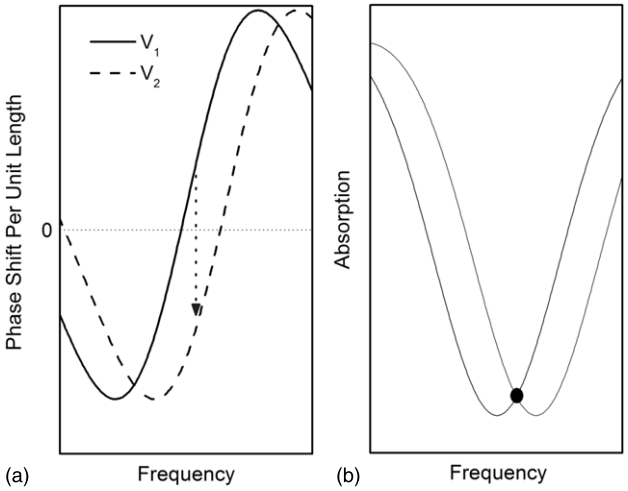

Figure 3. Illustration of an ultra-low Vπ Mach–Zehnder modulator based on a large material dispersion in a slow light device. (*a*) The characteristics of the phase shift per unit length. (*b*) the corresponding absorption. If the signal wavelength is chosen at the location of the black circle in (*b*) and when a voltage is applied to the slow light device to shift the energy level, the dispersion curve also shifts in frequency from the solid line to the dashed line as in (*a*). This shift creates a phase shift for the signal while keeping the absorption the same. Due to a large slope of the refractive index with respect to the frequency, the voltage required to shift the spectrum in order to generate the π-phase shift can be very small.

compared with an analogue modulated signal such as the radio frequency (RF) information carried by an optical wave in a microwave photonics system. We compare the requirements of these benchmarking parameters for applications in optical buffers, TTD in PAAs, pulse synchronization, all-optical signal processing and quantum information processing. Some of the applications require a large delay. In a packet switched network, a basic packet size is 424 bits which correspond to a total delay of 10 ns in a 40 Gbit s^{-1} network. For applications such as TTD in PAAs, the typical delay is a lot smaller. A delay of 90 ps is able to generate a steering range of $\pm 28^{\circ}$ [47].

Slow light generates the delay for the envelope of the field instead of the intensity and thus preserves its coherent (phase) information. This property allows slow light devices to be applied to a coherent communication network or quantum information processing where the phase information is crucial. In applications such as optical switching, slow light can generate a π-phase shift for an incoming optical pulse within a short distance by enhancing the nonlinear Kerr effect [54]. The large percentage shift of the refractive index over a narrow spectral range can also be applied to an ultra-efficient π-phase shifter even for a CW input. This gives slow light a good candidate in achieving an ultra-low V_π Mach–Zehnder modulator [55] as depicted in figure 3.

A slow light variable optical buffer has many advantages over an optical buffer that changes its delay by physically adjusting the optical path length. The latter case either mechanically changes the length of the optical path or recirculates the signal inside a loop for a controlled number of times. Recently, there have been a few proposals and demonstrations on how the change in optical path length can be achieved without any mechanical parts or recirculating controllers [56–58]. For example, Sharping *et al* [58] showed that the signal can be virtually routed to a 'different' optical path by changing its wavelength. By using a highly dispersive fibre segment, the signals at different wavelengths see different group velocities and therefore experience different amounts of delay. At the end of the delay line, the signal wavelength is shifted back to its original quantity. This approach, however, does not shrink the actual device size because the signal is still travelling at the same velocity as it is in the fibre delay loop. But it provides an interesting alternative for the design of a variable delay line in addition to the slow light based approach.

Ideally, we would want a slow light device to generate an arbitrarily large delay with an arbitrarily large operating bandwidth. Unfortunately this has been shown to be not possible in numerous reports [7, 59–63] whether for slow light devices based on material dispersion or on waveguide dispersion. For an ideal device, there is no absorption and the operating bandwidth is only limited by the dispersion characteristics of the slow light mechanism. The delay–bandwidth product $\Delta\tau B$ is determined by the amount of dispersion we can achieve which is given by [7, 59]

$$\Delta\tau B = L\frac{n_{\mathrm{avg}} - n_{\mathrm{min}}}{\lambda_0}, \tag{3}$$

where L is the device length and $n_{\mathrm{avg}} - n_{\mathrm{min}}$ is the maximum change in the refractive index that leads to slow light. In the extreme case where $n_{\mathrm{min}} \sim 0$, the delay–bandwidth product per unit length is given by $n_{\mathrm{avg}}/\lambda_0$ which is nothing but the optical wavelength in the material. In other words, the minimum device length required to store one bit of information is limited by the optical wavelength in the device. For a typical semiconductor material at 1.55 μm wavelength, $n_{\mathrm{avg}}/\lambda_0 = 3.6/1.55\mu$m and the minimum length to store a bit (L_{bit}) is 430 nm. To further scale down L_{bit}, we need to scale down the optical wavelength or increase n_{avg} but the latter will also increase the coupling loss to the slow light device due to the index mismatch to other optoelectronics components. It is interesting to compare (3) with optical storage and CMOS technologies in which the scaling also depends on the optical wavelength used for the read-out head and lithography, respectively.

It is worthwhile to note that in deriving (3), we have assumed that the amplitude response is constant throughout the spectral range in which we are interested. This is only possible for some special cases of waveguide dispersion based slow light devices. For material dispersion based slow light device, the amplitude response is determined by the overall absorption (or gain) spectrum and is linked to the refractive index dispersion via the KK relation. As we will show in the next section, the delay–bandwidth product of a material dispersion based device is always smaller than that of the ideal case (3) because of a non-flat amplitude response.

3. General principles of slow light in semiconductors

As we have discussed in the section 1, slow light can be achieved either with a large material dispersion or with a large waveguide dispersion. In semiconductor heterostructures,

Table 2. Comparison with material dispersion and waveguide dispersion based semiconductor slow light devices. The definitions of 'pros' and 'cons' here are solely based on an ideal slow light device that is universally suitable for all applications.

	Pros	Cons
Material dispersion	(1) A narrow spectral hole can be obtained by coherent processes including EIT and CPO and leads to a large slow down factor. (2) The width and the depth of the spectral hole can be dynamically tuned at a high speed. This leads to a high-speed operation. (3) Device structure can be as simple as a straight waveguide and can be made very compact.	(1) Coherent process is involved. (2) Device-to-device variation may be an issue for slow down factors. For non-ideal EIT and CPO devices, loss often becomes the limiting factor. (3) For devices using gain peaks instead of spectral holes, amplified spectral emission (ASE) and gain saturation need to be taken into account which limit the maximum slow down factor that can be achieved.
Waveguide dispersion	(1) Passive device does not involve any coherent process. (2) Mature semiconductor fabrication technology can be leveraged to make device-to-device variation small.	(1) It is difficult to quickly change the refractive index of a photonic crystal or resonator structure which results in a low operating speed. (2) The overall device size is bulky and complicated if a large slow down factor is desired.

large material dispersion can be achieved by inducing a narrow spectral transparency hole (or a gain peak). On the other hand, large waveguide dispersion can be achieved by using photonic crystal or resonator structures. A brief comparison between these two methods is given in table 2. Please note the definitions of 'pros' and 'cons' here are solely based on an ideal slow light device that is universally suitable for all applications. Some of the cons listed in the table may not present severe limitations for certain applications.

3.1. Material dispersion based slow light

In the case of material dispersion, a narrow spectral hole (or a narrow gain peak) is required to generate a steep dispersion of the refractive index. The slow down factor can be expressed in terms of the spectral characteristics of the transparency window according to (2). To further simplify the equation, we consider a symmetric spectral hole (or a symmetric gain peak) whose spectral characteristics can be expressed by a function $\Delta\alpha(\omega)$ defined as the difference between the original and modified absorption spectra. $\Delta\alpha(\omega)$ is taken to be positive at the centre of the spectral hole. If we Taylor expand $\Delta\alpha(\omega)$ around the centre frequency, we get

$$\Delta\alpha(\delta) = \Delta\alpha(0) - \frac{1}{2}\delta^2 \left|\frac{\mathrm{d}^2\Delta\alpha(\delta)}{\mathrm{d}\delta^2}\right|_{\delta=0} + \cdots, \tag{4}$$

where $\delta = \omega' - \omega$ is the detuning from the centre frequency. In the case of a single gain peak, we can replace $\Delta\alpha(\omega)$ with the gain profile $g(\omega)$ and the discussions below will remain the same. If the shape of the spectral hole is smooth enough, we can ignore all the higher order terms in (4) and the spectral hole can be approximated by resuming the series in (4) again. The result is a Lorentzian shape as follows:

$$\Delta\alpha(\delta) = \frac{\Delta\alpha(0)}{1 + \frac{1}{2}(|\Delta\alpha"(0)|/(\Delta\alpha(0))\delta^2} = \frac{\Delta\alpha(0)}{1 + (2\delta/\Delta\nu)^2}, \tag{5}$$

where $\Delta\nu$ is the FWHM of the spectral hole. Substituting (5) into (4), we get

$$S(\delta = 0) = n_{\mathrm{bac}} + c\frac{\Delta\alpha(0)}{\Delta\nu}. \tag{6}$$

This result confirms our assertion before that the slow down factor is inversely proportional to the width of the spectral hole and is proportional to the depth of the spectral hole. Note the derivation of (6) is independent of the physical mechanism of the slow light. The only assumption made was the spectral smoothness of the spectral hole. Experimentally (6) has been verified in semiconductor QWs with CPO [23]. From (6), we can further deduce the delay–bandwidth product of a material dispersion based slow light device to be

$$\Delta\tau\Delta\nu \simeq L\Delta\alpha(0), \tag{7}$$

where we have assumed the slow down factor is large enough that we can ignore the first term in (6). To relate the operating bandwidth B to the width of the spectral hole $\Delta\nu$, we note that the amplitude response of a material dispersion based slow light device is not flat. Instead, it is modified by the induced spectral hole via the KK relation. The amplitude response $T(\omega)$ is given by

$$T(\omega) \propto \exp[\Delta\alpha(\delta)L]. \tag{8}$$

We assume the operating bandwidth is limited by the amplitude response. This gives us an upper bound of the operating bandwidth because the slow down factor itself is a function of the detuning δ too as in (6). The 3-dB bandwidth of $T(\omega)$ and hence the operating bandwidth is given by

$$B = \Delta\nu\sqrt{\frac{\ln 2}{\Delta\alpha(0)L}}, \tag{9}$$

where (5) is used in obtaining (9). Note the square-root device length dependence of the operating bandwidth. This is a general property of a material dispersion based slow light device or a minimum phase filter (MPF) as will be discussed

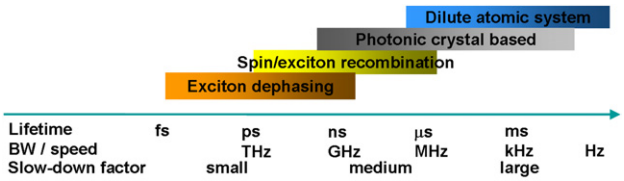

Figure 4. The comparison of lifetimes of a few typical physical processes in semiconductors with a dilute atomic system. The operating bandwidth (BW), the operating speed, and the slow down factor are also compared. The lifetime of a photonic crystal based structure is determined by its quality factor or photon lifetime.

in the next section. In these systems, the amplitude response and the phase response cannot be independently controlled. They are connected with each other via the KK relation or the Hilbert transform as in MPFs. The delay–bandwidth product for a material dispersion based slow light device can now be obtained by combining (7) and (9). The result is as follows:

$$\Delta\tau B = \sqrt{\ln(2)}\sqrt{L\Delta\alpha(0)} \qquad \text{or} \qquad \sqrt{\ln(2)}\sqrt{Lg(0)}. \tag{10}$$

This square root dependence has been numerically demonstrated in an EIT system using uniform semiconductor quantum dots [60]. Note the delay–bandwidth product per unit length is in general smaller than that of the ideal case (3) because of the square-root dependence on the device length. In obtaining (10), we did not consider other constraint factors for the operating bandwidth. Possible constraints include background absorption (or gain saturation and amplified spontaneous emission (ASE) noise in a gain system [64]) and signal distortion due to a non-constant slow down factor versus detuning. These issues will be, however, important in practical applications.

The width of the spectral hole is determined by the lifetime of the physical process involved. Figure 4 compares the lifetimes of a few typical physical processes in semiconductors with a dilute atomic system. The corresponding slow down factor, operating bandwidth and the operating speed are also plotted together. We can see that the semiconductor heterostructure provides a wide range of slow down factor. This cannot be easily achieved in other material systems such as optical fibres.

3.2. Waveguide dispersion based slow light

Similarly in the case of waveguide dispersion, a rapid change in the refractive index over space is necessary to generate a large and positive $\partial n/\partial\beta$ which leads to a large slow down factor according to (1). This can be achieved in a photonic crystal or a resonator structure. The waveguide dispersion based slow light structure has been widely used in microwave circuits where the terminology 'slow-wave' is often adopted [65]. For example a 'slow-wave' device can be inserted into an antenna to change the wave front and strengthen the energy directionality. Slow light devices based on waveguide dispersion are often not compact due to the space required to generate a sufficient refractive index change. This can be improved but not eliminated with a microresonator structure [62, 66, 67]. The waveguide dispersion structures can be

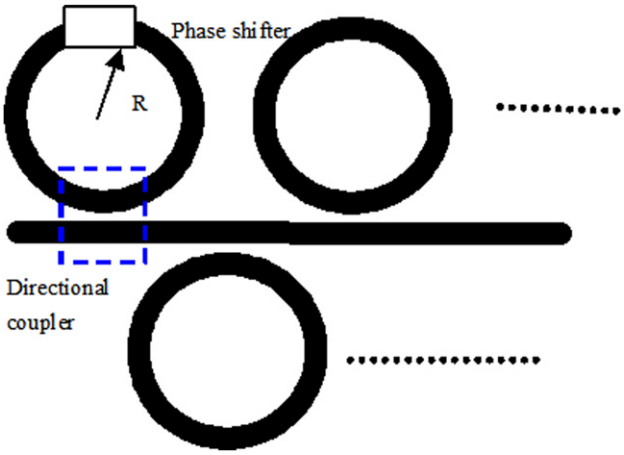

Figure 5. Schematic of a ring resonator based slow light device. The ring waveguide is coupled to the straight waveguide via a directional coupler which can be simply an air gap or filled with another lower refractive index material. Multiple rings can be cascaded to increase the total delay and improve the operating bandwidth if different rings have different radii. A phase shifter can be added to the ring waveguide to introduce an additional phase shift.

divided into two different categories [62]: the MPFs and non-MPFs. The difference between them is that the amplitude and phase responses of MPFs are governed by the Hilbert transform which is analogous to the KK relation in the material dispersion system while the amplitude and the phase responses can be independently controlled in a non-MPF structure. The simplest realization of a non-MPF filter is a ring or disk resonator as shown in figure 5 which has a unity amplitude response that is also independent of the signal wavelength. This type of filter is called an all-pass filter (APF) [68, 69]. An APF can be used as a fundamental building block for the slow light device to achieve a flat amplitude response while at the same time lower the group velocity. Because of the independent controllability of the amplitude response, a non-MPF slow light device has a delay–bandwidth product per unit length to be independent of the device length. This property is identical to an ideal device as in (3). However, the minimum length required to store a bit is about 6 times the microresonator dimension or 3 times the optical wavelength in the material [7]. Moreover, the system size to achieve a huge delay is often very large in order to accommodate the number of resonators required which is directly proportional to the delay–bandwidth product of the system. The overall system size can be reduced in some degree by embedding the material dispersion system into the waveguide dispersion structure [70]. This combination, however, will not change the delay–bandwidth product limitation.

3.3. Delay–bandwidth product trade-off

From the discussions so far, the delay–bandwidth product trade-off (3) or (10) is a universal limit for a general slow light device regardless of the physical mechanism involved. Different physical mechanisms give different delay–bandwidth products but they are all upper-bounded by (3). The question now is: Is there anyway to go around it? The answer is 'Yes' and the solution is to use multiple devices together.

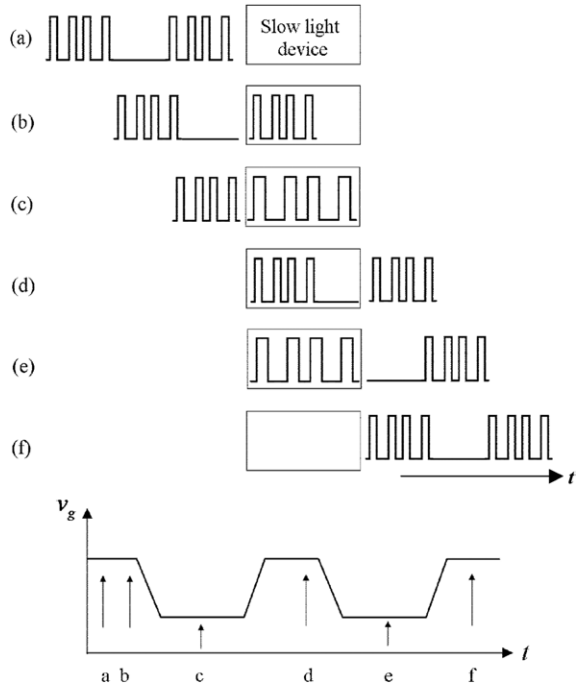

Figure 6. By adiabatically changing the group velocity of the slow light device, the signal that has entered the device spreads out in time and its bandwidth is effectively reduced. The total amount of delay can be increased due to the reduction of the bandwidth. The trade-off is the need for an extra hold-off time. Without the hold-off time, the following signal will overlap with the signal that is still in the device and results in information loss. This figure illustrates the signal evolution at different stages. The group velocity of the signal changes with time and is depicted at the bottom of the graph. The labels (*a*)–(*f*) correspond to the sub-figures (*a*)–(*f*), respectively. Once the packet enters the slow light device completely at time b, the group velocity is adiabatically reduced to spread out the signal in time (as shown in (*c*)) in order to reduce the effective bandwidth. After the signal accumulates the desired amount of delay and completely exits the device at time (*d*), the group velocity is resumed to its original value and the device is again ready for the next packet. This process can be repeated again for the next incoming packet.

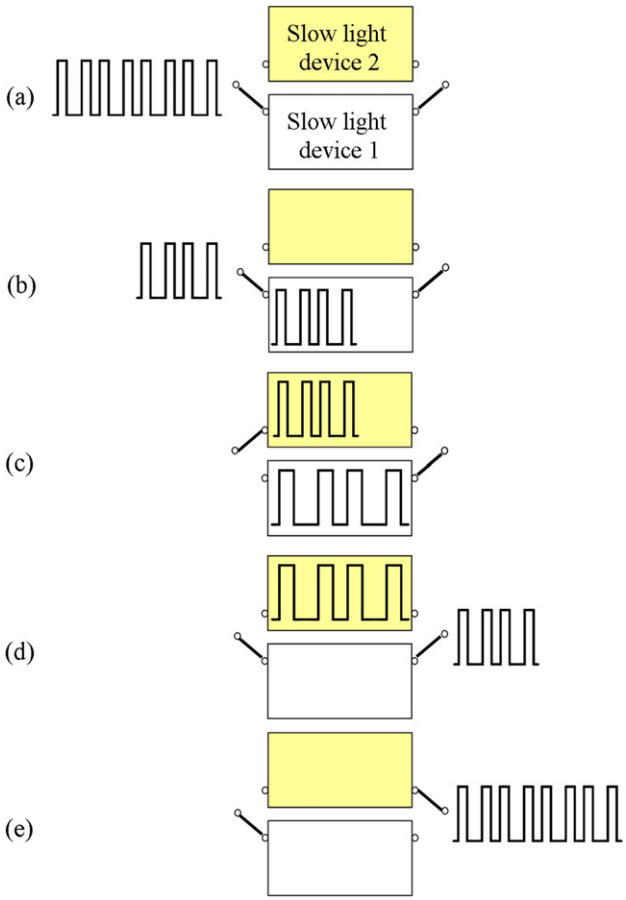

Figure 7. By using multiple slow light devices with a time demultiplexing switch, the hold-off time can be eliminated. The delay–bandwidth product limit can be increased by N-fold where N is the number of slow light devices used.

There are at least two ways in doing that. The first approach uses a time-variant slow down factor to dynamically change the signal bandwidth. To be clear, we consider an optical signal comprising of a chain of packets. Each packet consists of a fixed length of optical signal with a certain signal bandwidth B_S. Normally if the signal is continuously fed into the slow light device, we would expect a maximum delay given by $\Delta\tau_{\max} = C/B_S$ where C is the delay–bandwidth product associated with the physical mechanism used in this case. It seems from the first glance that it is impossible to get more delay with a fixed bandwidth. But as illustrated in figure 6, if we close the input port of the slow light device for a certain amount of time (hold-off time) after receiving the first packet, or if there is an interval between two adjacent packets, we can take advantage of the extra time window to spread out the received packet uniformly in time by adiabatically decreasing the group velocity. This approach effectively reduces the bandwidth of the packet. After the desired delay is accumulated, the group velocity of the signal is then adiabatically recovered to its original quantity. When the signal bandwidth is reduced at times (*c*) and (*e*) as in figure 6, the total amount of allowed delay is increased. This approach has been experimentally demonstrated to bring the light to stop in an atomic vapour [20] with EIT by gradually narrowing down the transparency window by turning down the intensity of the pump beam. It has also been theoretically analysed in a coupled resonator structure [66,71]. We should keep in mind that this approach does not, however, increase the delay–bandwidth product if only a single device is used. It merely puts the slow light device into a busy state after receiving the maximum allowed bandwidth and then recovers whenever it becomes idle again, that is, when the received packet has exited the device. We can, however, eliminate the hold-off time by using multiple slow light devices along with a time demultiplexing switch as shown in figure 7. Once the first device becomes busy (in this example device 1), we can immediately switch the signal to the next available device (device 2 in our example). By using N multiple devices in parallel, the overall delay–bandwidth product can be increased by $N-$fold.

Another scenario that addresses the delay–bandwidth product limit is to couple several slow light devices together, each with a slightly different operating wavelength [62, 72]. The coupling is such that the signal can interact with all individual devices simultaneously. This is similar to the tricks used in a filter design to flatten out the transfer function by using a higher-order transfer function. If each different signal wavelength component is appropriately routed into a

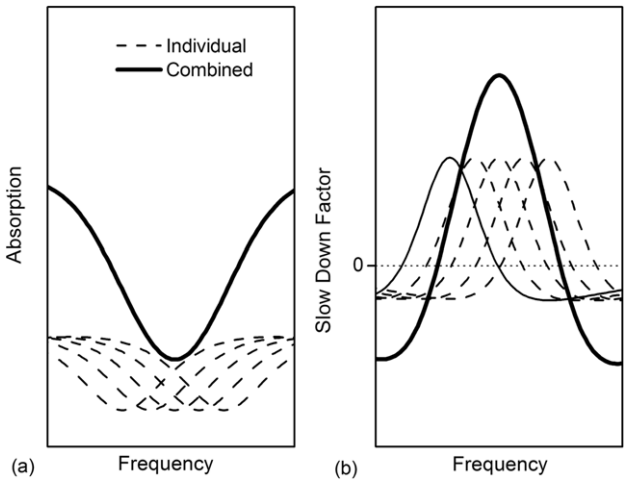

Figure 8. (*a*) The overall absorption and the (*b*) slow down factor (solid lines) of a coupled system that consists of five different slow light segments. Each segment (dashed lines) has a slightly different operating frequency (or wavelength) but all the segments interact with the signal simultaneously. To suppress the large absorption at frequencies farther away from the centre frequency, we use weighted average such that each segment contributes in a different percentage to the overall response. This can be achieved by adjusting the overlap of each segment with the signal. In this graph, the weights for segments from left to right (on the frequency axis) are 0.4, 0.7, 1.0, 0.7 and 0.4, respectively.

particular slow light segment that generates the same delay of $\Delta\tau$ as illustrated in figure 8, the total delay–bandwidth product can be greatly improved. This approach, however, increases the size of the system, power consumption and the design complexity in order to properly overlap the responses from different slow light segments to flatten out the over response. For example in figure 8, the contributions from different devices are weighted such that the larger absorption at frequencies farther away from the centre can be suppressed to maintain an overall flat response. This weighted average will compromise the overall slow down factor but is necessary to improve the overall system bandwidth. The coupling of multiple devices can also be applied to overcome the sample inhomogeneity existing in some structures such as in a self-assembled QDs array. Since each dot in the ensemble is different, the slow light characteristics of each dot may be different from each other and the overall slow light effect may be washed out. To overcome this issue, we can apply multiple pumps and effectively decouple the dots from each other. Using the same picture as described above and in figure 8, the net slow light response can be recovered. Again, this approach does not change the delay–bandwidth product limit of a single element. The increase of the delay–bandwidth product is achieved through the combination of multiple devices. This is similar to the above time-variant group velocity approach.

3.4. Fast light

Before we leave this section, it is interesting to note that in (6), if $\Delta\alpha(0)$ becomes negative, the slow down factor can become less than one or even negative. This corresponds to the superluminal light (fast light) and the negative group velocity, respectively. A negative $\Delta\alpha(0)$ corresponds either to a single absorption peak as in the case of Chu and Wong's experiment [8] or to a spectral hole in the gain background [27, 73, 74]. Fast light has long been a debate whether it violates the causality principle [75]. It is beyond the scope of this paper to discuss the debate but from the framework developed above, fast light is a continuous pulse reshaping process just like slow light. The difference of fast light from slow light is that the reshaping process takes place in an opposite direction due to an opposite sign of the dispersion term $\partial n/\partial\omega$ or $\partial n/\partial\beta$. The definition of signal velocity in the context of fast light, however, has to be defined in a more restrictive way. If it is defined by the onset of the signal based on the signal-to-noise ratio, the signal velocity will be different from the group velocity and its value will always be less than the speed of the light in the vacuum c [75]. But if it is defined by the location of the peak of the pulses, the group velocity can exceed c.

4. Several slow light mechanisms in semiconductors

In this section, we compare several slow light mechanisms in semiconductor heterostructures including EIT, CPO, gain systems, OIL and exciton dephasing. All these are material dispersion based systems with tuning capabilities on their slow down factors. The key parameters for these mechanisms are summarized in table 3.

4.1. Electromagnetically induced transparency

The first proposal of slow light in semiconductor heterostructures was to use EIT in a QD waveguide [1]. An EIT process involves a three-level system and two laser beams, one strong (pump) and one weak (signal) each couples to an allowed transition in the system. Depending on the relative configuration of the pump and the signal beams, an EIT process can be categorized into three different configurations: π, V and the ladder systems as shown in figure 9. Without the presence of the strong beam ω_p, the signal beam ω_s experiences a strong absorption due to resonant exciton excitations. Once we turn on the pump beam, the linkage of the two optical transitions through the non-radiative coherence between levels |3> and |1> creates a destructive interference and completely suppresses the possibility of any exciton excitation between levels |1> and |2>. Therefore the signal sees a spectral hole in the absorption spectrum. The absorption at the centre of the spectral hole has been shown to be extremely small due to the destructive quantum interference [78]. This deep and narrow spectral hole gives rise to slow light. The width of the spectral hole is given by the non-radiative coherence dephasing time. In semiconductors, there are different dephasing channels with very different coherence lifetimes. For example, the exciton dephasing is typically on the order of 100 fs or shorter in a semiconductor QW but the electron spin coherence between two degenerate conduction bands can be much longer. It has been shown that the electron spin coherence in a [110] GaAs/AlGaAs QW can be as long as 10 ns at RT [79]. EIT has been demonstrated in semiconductor QWs at 10 K [80, 81]. However, to the best of our knowledge there has not been any concrete report of EIT in semiconductors at RT.

Semiconductor self-assembled QDs are high quality, defect-free nanostructures that provide three-dimensional potential confinement for excitons. The strong confinement

Table 3. Comparison of different slow light mechanisms on their benchmarking parameters.

	S	$\Delta S/S$	B	Loss	Operating temperature
EIT [1]	10^2–10^7	$\gg 2$	THz	Small but still finite	10 K–RT
CPO [23–25]	10^2–10^4	1–2	MHz–GHz	Finite	10 K–RT
Gain system [31, 32, 34, 76, 77]	$1 \sim 10^3$		GHz–0.1 THz	No loss but has ASE noise	RT
OIL [36]	N/A	N/A	GHz band at high frequency	Both loss and gain are present at different frequencies	RT
Exciton dephasing [33]	10^3	2	>1 THz	Finite	20–80 K

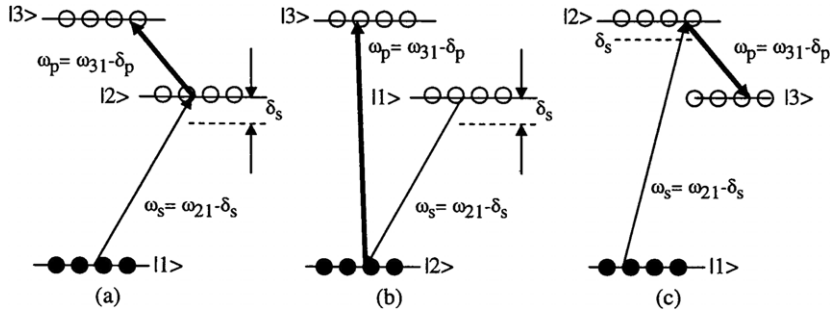

Figure 9. Schematics of three possible EIT configurations. (*a*) Ladder configuration (*b*) V configuration (*c*) π configuration. In all the cases, thick transition lines represent the strong pump fields and thin transition lines represent the weak signal fields. Open and filled circles represent the unpopulated and populated initial states, respectively.

makes the QDs array to resemble vital properties of atoms and makes them an ideal candidate for EIT. The exciton dephasing of a single QD has been observed to be around 7 μeV at low temperature and 4.5 meV at RT [82, 83], respectively. These correspond to spectral holes with widths around 1.7 GHz and 1 THz, respectively. The slow down factor in a uniform QDs array can be as large as 10^7 at low temperature according to figure 2.

The state of the art QDs array still exhibits a very large inhomogeneous broadening linewidth (20–60 meV), which is many times more than that of the homogeneous linewidth (4.54 meV at RT) of a single QD. The non-uniformity which is created during the self-assembly process of QDs fabrication makes the energy level fluctuating and washes out the overall slow light effect. As we have discussed previously, the inhomogeneity can be overcome by adopting a multiple-pump scheme [72]. So far, no experiments have demonstrated explicitly the slow light effect induced by EIT in semiconductor heterostructures.

4.2. CPO

4.2.1. CPO in QWs. CPO is a coherent energy transfer process between the pump and the signal beams in a two-level system as shown in figure 10. The pump and the signal beat at a frequency $\omega_p - \omega_s$. When the beating frequency is small enough that the carriers in the semiconductors can catch up with the oscillation back and forth between levels |1> and |2>, the carriers will generate a temporal grating and induce the energy exchange between the pump and the signal. This process, similar to EIT, creates a spectral hole

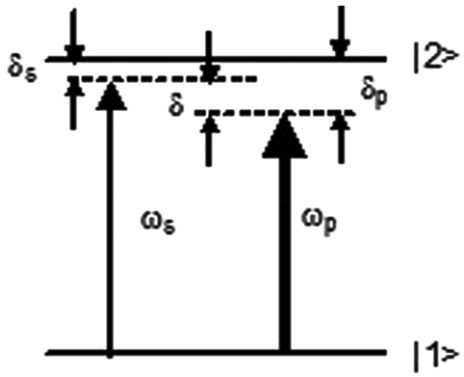

Figure 10. Schematic of CPO. The pump beam (represented by the thick line) and the signal beam (represented by the thin line) beat with each other and create a temporal grating at a frequency $\delta = \omega_p - \omega_s$.

seen by the signal and leads to slow light. Since the carrier recombination lifetime in semiconductors is on the order of ns, the width of the spectral is on the order of GHz. CPO has been experimentally demonstrated in a ruby crystal [84] and semiconductor QWs [44]. Slow light with CPO in semiconductor QWs has also been demonstrated in various experiments both at low temperature [23, 25] and RT [24]. A group velocity less than 200 m s^{-1} was demonstrated by direct time measurement [25].

The KK relation which lays the foundation of the theoretical framework developed in section 3 has been verified to be a good agreement in the CPO experiment. Figure 11(*a*) shows the phase delay βL and the absorption which are measured simultaneously in the experiment [23]. The phase

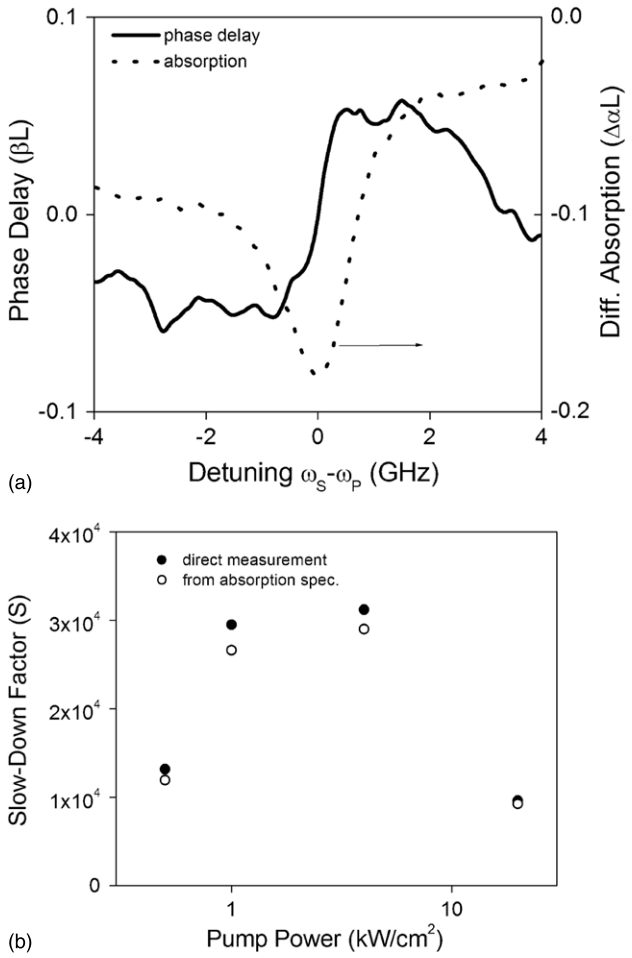

Figure 11. (*a*) The measured phase delay and the signal absorption as a function of the signal-pump detuning. These two quantities are measured simultaneously. The slope of the phase delay with respect to the detuning determines the slow down factor. In this case, the slow down factor is 31 200 and is a constant over a 2 GHz window. (*b*) The dependence of the slow down factor on the pump intensity. The filled and open circles represent direct measured values and values calculated from the KK relation, respectively. Good agreement between them verifies the theoretical framework developed in section 3.

delay is proportional to the refractive index and therefore its slope with respect to the detuning gives the slow down factor. In figure 11(*a*), the slow down factor is 31 200 and is constant over a 2 GHz window. If the KK relation is valid, the directly measured slow down factor should be equivalent to the value calculated from the width and the depth of the spectral hole in the absorption background. Figure 11(*b*) shows that this is indeed the case. The calculated slow down factor from the absorption spectrum agrees well with the direct measurement. When the pump intensity changes, the slow down factor also changes as shown in figure 11(*b*). The fractional change in the slow down factor is $\Delta S/S \sim 1.3$.

4.2.2. CPO in QDs. Since the frequency of the temporal grating only depends on the beating between the pump and the signal, the CPO process is immune to the sample non-uniformity [85]. In fact CPO has been demonstrated in an inhomogeneously broadened QD SOA [28, 85]. Both slow light and fast light have been observed by changing the bias voltage to the QD SOA. There are three regimes of operation for a p–n junction SOA:

(1) When the device is reverse-biased, it is essentially an electro-absorption modulator, the CPO effects result in a slow light.
(2) When the device is under a forward bias current below the transparent current level, where the optical gain is equal to the background absorption, the overall waveguide is still absorptive, slow light is observed using CPO.
(3) When the forward bias current is above the transparent current level, the net modal gain of the SOA is positive, CPO results in fast light phenomena.

All three regimes of operation have been demonstrated at RT. In the experiment, the active region of the device consists of ten stacks of InAs/GaAs QDs with p-type doping in the GaAs barriers and has a total thickness of 388 nm. The top and bottom optical cladding layers are grown with 1500 nm of $Al_{0.35}Ga_{0.65}As$. Electroluminescence spectra show two peaks close to 1290 nm and 1210 nm, corresponding to the ground state and excited state emissions, respectively. The length of the QD SOA is about 700 μm. The heat-sink temperature is controlled to stay at 20 °C.

A phase shift technique [86] is used to measure the changes of the gain/absorption and the slow down factor in the QD SOA under optical pump and current injection. In the experimental setup [27, 28], the pump and signal are counter propagating inside the device. The signal is a tunable laser source and is followed by an optical isolator to avoid external feedbacks. A network analyzer is used, functioning like a lock-in amplifier with high-speed chopping frequency, to determine the signal delay. A polarization controller to match the polarization of the modulator is built into the network analyzer (NA). The radio frequency (RF) modulated output from the NA is fed into the optical circulator which functions as an optical isolator to the signal and as the port of the transmission measurement for the pump beam from the opposite direction. A two-lens coupling system is used to couple the light into and out from the QD SOA with an estimated coupling loss of 12 dB on each side. Two polarization controllers are used to align the polarizations of the pump and signal with the dominant TE polarization of the QD absorption. The signal transmitted through the QD SOA is fed back to the network analyzer to measure the phase delay and gain of the RF modulated signal. The transmitted pump is used to monitor and correct the drift of the optical coupling systems.

First, we obtain signal transmission spectra of the QD SOA without the presence of pump, as shown in figure 12. We observe reduced absorption (or increase in gain) when we raise the forward injection current from 0 mA to the transparency current of 30 mA due to the electron–hole occupations. We also observe clear electro-absorption effects in the reverse bias region ($V < 0$) with sharp QD bound state absorption. The increase in absorption with increasing reverse bias voltage is especially visible near the ground of the QDs. This is due to the fact that the sample is p-type doped, therefore, an increase in the reverse bias depletes the hole occupation and increases the absorption. Between 0 and 30 mA, the device functions as an absorptive medium with maximum absorption at 0 mA and decreasing towards transparency (zero absorption) at 30 mA.

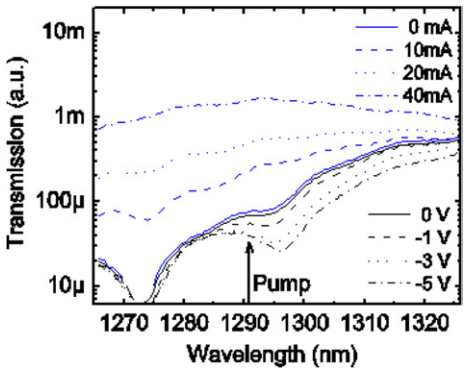

Figure 12. Transmission spectra of the QD SOA under forward (up to transparency current = 30 mA) and reverse bias. The spectra under forward bias indicate carrier injection or band filling of QD states, whereas those under reverse bias show a large absorption near ground and excited states.

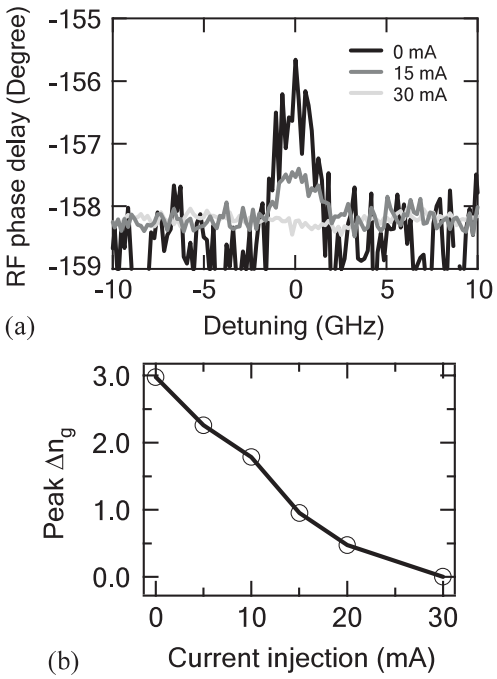

Figure 13. (*a*) The spectra of the RF phase delay (or the change in group index) as a function of the detuning between the pump and signal frequency at three bias currents: 0, 15 and 30 mA. (*b*) The peak group-index change is plotted as a function of the current injection into the QD SOA. The optical pump is fixed at 0.3 mW (inside the device). After [28].

Therefore, slow light effect is expected within this range of operation current.

Figure 13(*a*) shows the measured slow down factor change (i.e. group index change or Δn_g in the figure) as a function of detuning for three bias currents at 0, 15 and 30 mA. In figure 13(*b*), we present the dependence of the peak slow down factor change as a function of the injection current into the 700 μm long device. The peak slow down factor change decreases as the current injection increases. As the current increases towards the transparency point (30 mA), the optical pump beam inverts less carrier population and consequently generates a weaker temporal grating and CPO. For current injection larger than 30 mA and up to 80 mA, no change in slow down factor was observed in this device. This could be attributed to the increasing intraband multi-carrier effect as the carrier density increases.

At zero voltage or 0 mA bias, the slow light effect is the largest. The phase change in 2° at 1 GHz corresponds to 5.6 ps delay or a group index change in 2.4 and a slow down factor of 4.8 relative to the vacuum. As the injection current is increased in the forward bias regime (yet below the transparency current of 30 mA, where the net gain/absorption is zero), the net QD SOA absorption is reduced because of the injection of electron–hole pairs. Therefore the slow down factor decreases. In the reverse bias regime, as the bias is changed from 0 to −3 V, it was observed a reduction of slow light even though the background absorption (see figure 11) increases. This is likely due to the fast carrier sweep-out of the QDs under a reverse bias field, resulting in a shorter T_1 interband carrier life time and a broader bandwidth (determined by $1/T_1$ and the Rabi frequency determined by the pump intensity). We have also achieved optical control of slow light by a factor of 2 or a group index change in 3.0 by varying the optical pump power.

4.3. Gain systems

As discussed in section 3, either a spectral hole inside an absorption background or a gain peak can lead to slow light. A gain system has been used to induce slow light in semiconductors [31, 32, 34, 76, 77]. The simplest gain system is just a single gain peak such as in the case of SRS. In a SOI waveguide, the width of the gain spectrum generated by SRS is on the order of 100 GHz [31]. The corresponding slow down factor is only about 3 mainly because of a small gain achievable in SRS. On the other hand, VCSEL operating in the amplifier regime provides a narrower gain spectrum and therefore a larger slow down factor. Delays at different signal frequency components are, however, non-uniform which may impact some applications. A delay up to ∼100 ps has been obtained in the experiment [32].

In SOA, if the pump and the signal beams are both injected into the waveguide, not only will there be CPO as described above but there will also be an induced dispersion due to nonlinear wave mixing effects [34, 77]. This wave mixing effect leads to an extra contribution on slow light. All the gain systems are subject to the constraints of gain saturation and ASE noise [31].

4.4. Optical injection locking

Using ultra-strong optical injection technique, delay–bandwidth product value of 1.0 was recently reported for a high-speed modulated signal, with the highest speed obtained being ∼16 GHz [36]. For over twenty years, OIL has been studied for a wide range of applications in optical communications, optical signal processing and microwave photonics [87–89]. Typically, the injection locking configuration uses one continuous-wave (CW) operated laser as the master laser to optically lock a second directly-modulated slave laser. This technique has been shown to be very effective to improve various modulation characteristics of the slave laser, including a reduced frequency chirp leading to an improved digital transmission [90], a significant increase in

the modulation frequency response [91] and greatly reduced nonlinear distortion [91].

Recently, a novel OIL scheme using a directly-modulated master laser and a CW slave laser was reported [36]. A full 2π phase shift is achieved at modulation frequency above a certain critical frequency f_c determined by the injection power ratio. This phase shift is effectively a slow/fast light medium and may be interesting for optical delay applications.

The group velocity of a laser cavity (herein slave laser) is strongly effected by its threshold gain. Under injection locking, i.e. when the slave laser is subjected to the injection of a strong CW light source, the slave laser's lasing wavelength is pinned by the master laser. Due to the stimulated emission from the master laser, the gain required by the slave laser is greatly reduced in value. Thus, the carrier density is reduced, which red-shifts the slave cavity (due to a non-zero linewidth enhancement factor or alpha-parameter).

In [36], two RT operated VCSELs at 1.55 μm were used as the master and slave lasers. The master laser is modulated with a single-tone sinusoidal signal, creating two side bands. The optical carrier frequency acts as the CW master line that locks the slave laser wavelength and shifts its cavity spectrum. The side bands thus experience different phases through the slave laser cavity, resulting in a time advance or delay of the sinusoidal signal. Total delay as much as 2π is achieved for a frequency range from 9.2 to 16 GHz, as shown in figure 14. Both absorption and gain exist but at different frequencies. Tunable delay can be achieved by changing the detuning or the drive current.

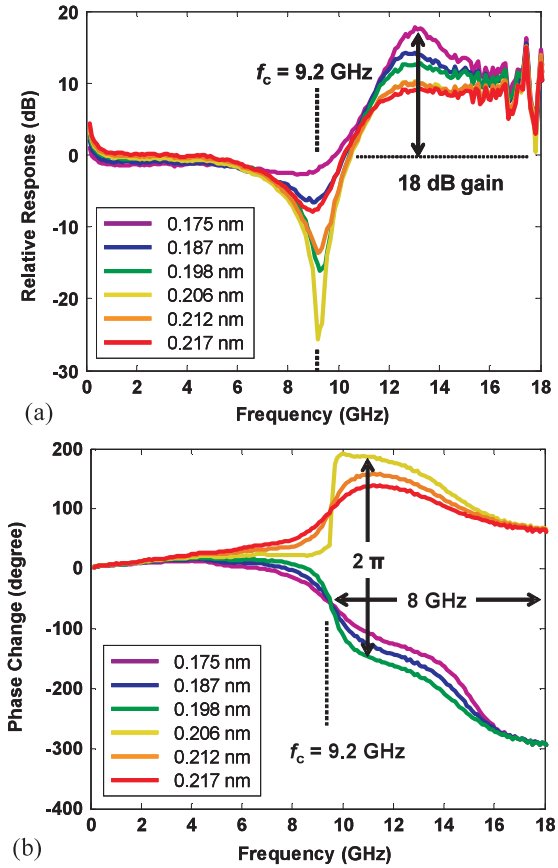

Figure 14. (*a*) Calibrated amplitude response of a modulated-master OIL VCSEL under a fixed injection power at various detuning values. (*b*) Phase change response of a modulated-master OIL VCSEL under a fixed injection power at various detuning values.

4.5. Exciton Dephasing

In this scheme [33], slow light is induced by the spectral hole between the two closely spaced heavy-hole and light-hole exciton absorption peaks. The spectral characteristics of these two exciton absorption peaks can be modified by free carrier injection due to their strong Coulomb interaction with excitons. Because of these changes, the depth of the spectral hole is also changed which results in the change in the slow down factor. $\Delta S/S > 2$ was reported with an 8 ps optical pulse propagating through GaAs/AlGaAs multiple QWs.

5. Conclusion

We have summarized the research activities of slow light in semiconductor heterostructures in recent years and presented a unified theoretical framework to compare different slow light mechanisms. We adopted an application oriented approach and hope in this way, readers from the applications side can gain more understanding on the advantages as well as disadvantages of a semiconductor slow light device for his/her favourite application. The general principles of slow light in semiconductor heterostructures were given. The principle we presented can be directly applied to other material systems including atomic gases and optical fibres.

Slow light slows down the propagation of information carried by an amplitude-modulated optical signal. When the signal distortion is small enough that all the useful information can be extracted at the output of the slow light device, the propagation velocity of the signal is equal to its group velocity and is given by (1). Two approaches including material dispersion and waveguide dispersion are possible to realize a slow light device and in both cases, the delay–bandwidth product per unit length has an upper bound which is equal to the optical wavelength in the material. In the material dispersion case, the dispersion of the material can be increased either electrically or optically. The increased dispersion generates a rapid change in the refractive index over a narrow spectral range and leads to slow light. The amplitude response is also modified at the same time the dispersion is changed and is governed by the KK relation. The resulted delay–bandwidth product $\Delta\tau B$ per unit length is smaller than that in the ideal case. $\Delta\tau B$ is proportional to the square root of the device length as well as the square root of the depth of the spectral hole (or the maximum gain in a gain peak.) In the case of waveguide dispersion, the amplitude response of a non-MPF can be separately controlled from its phase response and results in a delay–bandwidth product approaching the ideal case. The trade-off we have to pay is a much larger system footprint in order to achieve a large slow down factor. On the other hand, the change in the slow down factor in a waveguide dispersion based slow light device is typically very slow.

We also discussed possible approaches to overcome the delay–bandwidth product limit by coupling multiple slow light devices together to either increase the overall bandwidth or dynamically decrease the signal bandwidth in each device to

result in more delay. The dynamic decrease in the signal bandwidth can be achieved by using multiple devices in parallel with a time demultiplexing switch. On the other hand, the coupling can be achieved either by physical coupling of different devices or by using multiple-pump beams in a non-uniform sample that exhibits a large inhomogeneous linewidth such as in QDs.

We compared several experimental demonstrations of slow light in semiconductor heterostructures with different physical mechanisms including EIT, CPO, gain system, OIL and exciton dephasing. All these are material dispersion based devices with a slow down factor that can be tuned at a high speed. The slow down factor achieved by a waveguide dispersion based structure is still rather limited owing to the fabrication complexity. Recently, a slow down factor of 125 was reported in a two-dimensional photonic crystal structure [38].

The main difference among these physical mechanisms we discussed is the width of the spectral hole which is directly related to the time constant of the physical process involved. EIT with excitonic coherence at RT and SRS involve fast exciton and phonon interactions, respectively. Therefore they provide a large operating bandwidth (∼THz) and a fast operating speed while at the expense of a small slow down factor. EIT with electron spin coherence and CPO involve slower processes that give an operating bandwidth ∼GHz and a slow down factor on the order of 10^3–10^4. OIL-VCSEL has both absorption and gain signatures at different frequency bands. The slow down factor versus signal modulation frequency is not linear which may limit some of its applications. On the other hand, the total delay in CPO is limited by the finite absorption and in SOA or other gain systems, by the gain saturation and the ASE noise.

We have also shown that regardless of the physical mechanism involved, the performance of all the material dispersion based slow light devices is eventually limited by the device length with or without the presence of these non-ideal factors such as loss and ASE noise. In spite of this limitation, the total amount of fractional delay we can achieve in a material dispersion based slow light device is given by

$$\frac{\Delta\tau}{\tau_p} = \lambda_m \Delta\alpha(0), \tag{11}$$

where $\tau_p \sim 1/B$ is the pulse width and λ_m is the optical wavelength in the material. For $\lambda_m = 1.55\,\mu\text{m}/3.6 = 430\,\text{nm}$ and $\Delta\alpha(0) = 10^4\,\text{cm}^{-1}$, this corresponds to a total fractional delay on the order of one pulse length! Despite of the small fractional delay, the variability of the slow down factor as large as 2 has been demonstrated in the exciton dephasing experiment. It already promises the slow light application in a PAA system [47]. To generate a more fractional delay, we need to create a deeper spectral hole in a highly absorptive material. Although slow light via EIT has not been demonstrated in semiconductors yet, it still promises the largest fractional delay compared with other physical mechanisms. For example for EIT in a uniform QDs array, the numerical simulation showed a fractional delay of 100 pulses is achievable.

There are still great challenges ahead for slow light to become a real solution for applications such as optical buffers in a telecommunication network or all-optical signal processing. They likely need an EIT based slow light device with electron spin coherence at RT. But nevertheless slow light has already shown great promises in some of other applications including a tunable TTD element in a PAA, ultra-low Vπ Mach–Zehnder modulators, pulse synchronization and ultra-compact low-light level nonlinear optical devices.

Acknowledgments

The authors would like to thank Hailin Wang at the University of Oregon, and Shu-Wei Chang, P Kondratko, M Fisher and H Su at UIUC for technical discussions on the physics of population oscillation. Part of this work is supported by the DARPA University Photonics Centre under grant No DARPA UCB SA4472-32446 and grant No AF SA3631-22549.

References

[1] Ku P C, Chang-Hasnain C J and Chuang S L 2002 Variable semiconductor all-optical buffer *Electron. Lett.* **38** 1581–3
[2] Harris S E and Hau L V 1999 Nonlinear optics at low light levels *Phys. Rev. Lett.* **82** 4611
[3] Fisher M R and Chuang S-L 2005 Variable group delay and pulse reshaping of high bandwidth optical signals *IEEE J. Quantum Electron.* **41** 885–91
[4] Chang-Hasnain C J, Ku P-C, Kim J and Chuang S-l 2003 Variable optical buffer using slow light in semiconductor nanostructures *Proc. IEEE* **91** 1884–97
[5] Jemison W D, Yost T and Herczfeld P R 1996 Acoustooptically controlled true time delays: experimental results *IEEE Microw. Guided Wave Lett.* **6** 283–5
[6] Ku P C 2003 Semiconductor slow-light device *PhD Dissertation* University of California, Berkeley
[7] Tucker R S, Ku P-C and Chang-Hasnain C J 2005 Slow-light optical buffers: capabilities and fundamental limitations *J. Lightwave Technol.* **23** 4046–66
[8] Chu S and Wong S 1982 Linear pulse propagation in an absorbing medium *Phys. Rev. Lett.* **48** 738
[9] Ogawa K, Katsuyama T and Nakamura H 1988 Time-of-flight measurement of excitonic polaritons in a GaAs/AlGaAs quantum well *Appl. Phys. Lett.* **53** 1077–9
[10] Hegarty J 1982 Effects of hole burning on pulse propagation in GaAs quantum wells *Phys. Rev.* B **25** 4324
[11] Ulbrich R G and Fehrenbach G W 1979 Polariton wave packet propagation in the exciton resonance of a semiconductor *Phys. Rev. Lett.* **43** 963
[12] Shaw N, Stewart W J, Heaton J and Wight D R 1999 Optical slow-wave resonant modulation in electro-optic GaAs/AlGaAs modulators *Electron. Lett.* **35** 1557–8
[13] Eggleton B J, Martijn de Sterke C and Slusher R E 1999 Bragg solitons in the nonlinear Schrodinger limit: Experiment and theory *J. Opt. Soc. Am. B: Opt. Phys.* **16** 587
[14] Wang S, Erlig H, Fetterman H R, Yablonovitch E, Grubsky V, Starodubov D S and Feinberg J 1998 Group velocity dispersion cancellation and additive group delays by cascaded fiber Bragg gratings in transmission *IEEE Microwave Guided Wave Lett.* **8** 327–9
[15] Scalora M *et al* 1996 Ultrashort pulse propagation at the photonic band edge: Large tunable group delay with minimal distortion and loss *Phys. Rev.* E **54** R1078
[16] Field J E, Hahn K H and Harris S E 1991 Observation of electromagnetically induced transparency in collisionally broadened lead vapor *Phys. Rev. Lett.* **67** 3062
[17] Boller K J, Imamolu A and Harris S E 1991 Observation of electromagnetically induced transparency *Phys. Rev. Lett.* **66** 2593
[18] Hau L V, Harris S E, Dutton Z and Behroozi C H 1999 Light speed reduction to 17 metres per second in an ultracold atomic gas *Nature* **397** 594–8

[19] Kash M M, Sautenkov V A, Zibrov A S, Hollberg L, Welch G R, Lukin M D, Rostovtsev Y, Fry E S and Scully M O 1999 Ultraslow group velocity and enhanced nonlinear optical effects in a coherently driven hot atomic gas *Phys. Rev. Lett.* **82** 5229

[20] Phillips D F, Fleischhauer A, Mair A, Walsworth R L and Lukin M D 2001 Storage of light in atomic vapor *Phys. Rev. Lett.* **86** 783

[21] Turukhin A V, Sudarshanam V S, Shahriar M S, Musser J A, Ham B S and Hemmer P R 2001 Observation of ultraslow and stored light pulses in a solid *Phys. Rev. Lett.* **88** 023602

[22] Bigelow M S, Lepeshkin N N and Boyd R W 2003 Observation of ultraslow light propagation in a ruby crystal at room temperature *Phys. Rev. Lett.* **90** 113903

[23] Ku P C, Sedgwick F, Chang-Hasnain C J, Palinginis P, Li T, Wang H, Chang S-W and Chuang S-L 2004 Slow light in semiconductor quantum wells *Opt. Lett.* **29** 2291–3

[24] Palinginis P, Sedgwick F, Crankshaw S, Moewe M and Chang-Hasnain C J 2005 Room temperature slow light in a quantum-well waveguide via coherent population oscillation *Opt. Express* **13** 9909–15

[25] Palinginis P, Crankshaw S, Sedgwick F, Kim E-T, Moewe M, Chang-Hasnain C J, Wang H and Chuang S-L 2005 Ultraslow light (< 200 m/s) propagation in a semiconductor nanostructure *Appl. Phys. Lett.* **87** 171102

[26] Mork J, Kjaer R, Van Der Poel M and Yvind K 2005 Slow light in a semiconductor waveguide at gigahertz frequencies *Opt. Express* **13** 8136–45

[27] Su H and Chuang S L 2006 Room temperature slow and fast light in quantum-dot semiconductor optical amplifiers *Appl. Phys. Lett.* **88** 061102

[28] Su H and Chuang S L 2006 Room-temperature slow light with semiconductor quantum-dot devices *Opt. Lett.* **31** 271–3

[29] Liang J Q, Katsuragawa M, Kien F L and Hakuta K 2002 Slow light produced by stimulated Raman scattering in solid hydrogen *Phys. Rev.* A **65** 031801

[30] Okawachi Y, Bigelow M S, Sharping J E, Zhu Z, Schweinsberg A, Gauthier D J, Boyd R W and Gaeta A L 2005 Tunable all-optical delays via Brillouin slow light in an optical fiber *Phys. Rev. Lett.* **94** 153902

[31] Okawachi Y, Foster M A, Sharping J E, Gaeta A L, Xu Q and Lipson M 2006 All-optical slow-light on a photonic chip *Opt. Express* **14** 2317–22

[32] Zhao X, Palinginis P, Pesala B, Chang-Hasnain C J and Hemmer P 2005 Tunable ultraslow light in vertical-cavity surface-emitting laser amplifier *Opt. Express* **13** 7899–904

[33] Sarkar S, Guo Y and Wang H 2006 Tunable optical delay via carrier induced exciton dephasing in semiconductor quantum wells *Opt. Express* **14** 2845–50

[34] Su H, Kondratko P and Chuang S L 2006 Electrically and optically controllable optical delay in a quantum-well semiconductor optical amplifier *Conf. on Lasers and Electro-Optics/Quantum Electronics and Laser Science (CLEO/QELS, Long Beach, CA, USA)* (Piscataway, NJ: IEEE)

[35] Qhman F, Yvind K and Mork J 2006 Slow light at high frequencies in an amplifying semiconductor waveguide *Conf. on Lasers and Electro-Optics/Quantum Electronics and Laser Science (CLEO/QELS, Long Beach, CA, USA)* (Piscataway, NJ: IEEE)

[36] Zhao X, Zhou Y, Chang-Hasnain C, Hofmann W and Amann M C 2006 Slow and fast light using master-modulate injection-locked VCSELs. *Conf. on Lasers and Electro-Optics/Quantum Electronics and Laser Science (CLEO/QELS, Long Beach, CA, USA)* (Piscataway, NJ: IEEE)

[37] Podivilov E, Sturman B, Shumelyuk A and Odoulov S 2003 Light pulse slowing down up to 0.025 cm/s by photorefractive two-wave coupling *Phys. Rev. Lett.* **91** 083902

[38] Altug H and Vuckovic J 2005 Experimental demonstration of the slow group velocity of light in two-dimensional coupled photonic crystal microcavity arrays *Appl. Phys. Lett.* **86** 111102

[39] Vlasov Y A, O'Boyle M, Hamann H F and McNab S J 2005 Active control of slow light on a chip with photonic crystal waveguides *Nature* **438** 65–9

[40] Notomi M N M, Yamada K Y K, Shinya A S A, Takahashi J T J, Takahashi C T C and Yokohama I Y I 2001 Extremely large group-velocity dispersion of line-defect waveguides in photonic crystal slabs *Phys. Rev. Lett.* **87** 253902

[41] Boyd R W, Gauthier D J and Gaeta A L 2006 Applications of slow light in telecommunications *Opt. Photon. News* **17** 19–23

[42] Chiao R Y and Milonni P W 2002 Fast light, slow light *Opt. Photon. News.* **13** 26–30

[43] Matsko A B, Kocharovskaya O, Rostovtsev Y, Welch G R, Zibrov A S and Scully M O 2001 Slow, ultraslow, stored and frozen light *Adv. At. Mol. Opt. Phys.* **46** 191–242

[44] Wang H, Jiang M and Steel D G 1990 Measurement of phonon-assisted migration of localized excitons in GaAs/AlGaAs multiple-quantum-well structures *Phys. Rev. Lett.* **65** 1255

[45] Willner A E, Zhang L, Luo T, Yu C, Zhang W and Wang Y 2006 Data bit distortion induced by slow light in optical communication systems *Conf. on Advanced Optical and Quantum Memories and Computing III, Proc. SPIE* **6130** 61300T-1

[46] Ku P C, Chang-Hasnain C and Tucker R S 2005 Link performance of all-optical buffers using slow light *Optical Fiber Communication Conf. (Long Beach, CA, USA)* (Piscataway, NJ: IEEE)

[47] Ng W, Walston A A, Tangonan G L, Lee J J, Newberg I L and Bernstein N 1991 The first demonstration of an optically steered microwave phased array antenna using true-time-delay *J. Lightwave Technol.* **9** 1124–31

[48] Yao S, Mukherjee B and Dixit S 2000 Advances in photonic packet switching: an overview *IEEE Commun. Mag.* **38** 84–94

[49] Hunter D K, Chia M C and Andonovic I 1998 Buffering in optical packet switches *J. Lightwave Technol.* **16** 2081–94

[50] Sakamoto T, Okada A, Hirayama M, Sakai Y, Moriwaki O, Ogawa I, Sato R, Noguchi K and Matsuoka M 2002 Optical packet synchronizer using wavelength and space switching *Photon. Technol. Lett. IEEE* **14** 1360–2

[51] Jespersen N V and Herczfeld P R 1990 Optical techniques for reconfiguring microwave phased arrays *IEEE Trans. Antennas Propag.* **38** 1054–8

[52] Hunter D B and Minasian R A 1997 Photonic signal processing of microwave signals using an active-fiber Bragg-grating-pair structure *IEEE Microw. Theory Tech.* **45** 1463–6

[53] Fleischhauer M and Lukin M D 2002 Quantum memory for photons: dark-state polaritons *Phys. Rev.* A **65** 022314

[54] Soljacic M, Johnson S G, Fan S, Ibanescu M, Ippen E and Joannopoulos J D 2002 Photonic-crystal slow-light enhancement of nonlinear phase sensitivity *J. Opt. Soc. Am. B: Opt. Phys.* **19** 2052–9

[55] Ku P C, Chrostowski L and Chang-Hasnain C J 2004 A novel, low Vpi-L BIT based optical modulators. *IEEE MTT (Ogunquit, ME, USA)* New York, NY: Institute of Electrical and Electronics Engineers USA pp 97–100

[56] Van Howe J and Xu C 2005 Ultrafast optical delay line by use of a time-prism pair *Opt. Lett.* **30** 99–101

[57] Van Howe J and Xu C 2005 Ultrafast optical delay line using soliton propagation between a time-prism pair *Opt. Express* **13** 1138–43

[58] Sharping J E, Okawachi Y, Van Howe J, Xu C, Wang Y, Willner A E and Gaeta A L 2005 All-optical, wavelength and bandwidth preserving, pulse delay based on parametric wavelength conversion and dispersion *Opt. Express* **13** 7872–7

[59] Tucker R S, Ku P C and Chang-Hasnain C J 2005 Delay-bandwidth product and storage density in slow-light optical buffers *Electron. Lett.* **41** 208–9
[60] Sedgwick F G, Chang-Hasnain C J, Ku P C and Tucker R S 2005 Storage-bit-rate product in slow-light optical buffers *Electron. Lett.* **41** 1347–8
[61] Khurgin J B 2005 Optical buffers based on slow light in electromagnetically induced transparent media and coupled resonator structures: comparative analysis *J. Opt. Soc. Am. B: Opt. Phys.* **22** 1062–74
[62] Lenz G, Eggleton B J, Madsen C K and Slusher R E 2001 Optical delay lines based on optical filters *IEEE J. Quantum Electron.* **37** 525–32
[63] Boyd R W, Gauthier D J, Gaeta A L and Willner A E 2005 Maximum time delay achievable on propagation through a slow-light medium *Phys. Rev.* A **71** 023801
[64] Uskov A V, Sedgwick F G and Chang-Hasnain C J 2006 Delay limit of slow light in semiconductor optical amplifiers *IEEE Photonic. Technol. Lett.* **18** 731–3
[65] Pierce J R 1950 *Travelling-Wave Tubes* (Princeton, NJ: Van Nostrand)
[66] Xu Y, Yariv A, Gunn C, Lee R K and Scherer A 2000 Tunable group velocity reduction in coupled-resonator optical waveguide (CROW) *Conf. on Lasers and Electro-Optics/Quantum Electronics and Laser Science (CLEO/QELS, San Francisco, CA, USA)* (Piscataway, NJ: IEEE) pp 93–4
[67] Melloni A, Morichetti F and Martinelli M 2003 Linear and nonlinear pulse propagation in coupled resonator slow-wave optical structures *Opt. Quantum Electron.* **35** 365–79
[68] Lenz G and Madsen C K 1999 General optical all-pass filter structures for dispersion control in WDM systems *J. Lightwave Technol.* **17** 1248–54
[69] Madsen C K, Lenz G, Bruce A J, Cappuzzo M A, Gomez L T, Nielsen T N, Adams L E and Brenner I 1999 An all-pass filter dispersion compensator using planaar waveguide ring resonators *Optical Fiber Communication Conf. (San Diego, CA, USA)* (Piscataway, NJ: IEEE)
[70] Ku P C, Chang-Hasnain C, Kim J and Chuang S L 2003 Semiconductor all-optical buffers using quantum dots in resonator structures *Optical Fiber Communication Conf. (Atlanta, GA, USA)* (Piscataway, NJ: IEEE)
[71] Yanik M F and Fan S 2004 Stopping light all optically *Phys. Rev. Lett.* **92** 083901
[72] Ku P C, Chang-Hasnain C J, Kim J and Chuang S L 2003 Slow-light in nonuniform quantum dot waveguide *IEEE Laser and Electro-Optical Society Annual Meeting (Tucson, AZ, USA)* (Piscataway, NJ: IEEE) pp 441–2
[73] Steinberg A M and Chiao R Y 1994 Dispersionless, highly superluminal propagation in a medium with a gain doublet *Phys. Rev.* A **49** 2071
[74] Chang H and Smith D D 2005 Gain-assisted superluminal propagation in coupled optical resonators *J. Opt. Soc. Am. B: Opt. Phys.* **22** 2237–41
[75] Kuzmich A, Dogariu A, Wang L J, Milonni P W and Chiao R Y 2001 Signal velocity, causality, and quantum noise in superluminal light pulse propagation *Phys. Rev. Lett.* **86** 3925
[76] Sun D and Ku P C 2006 Slow light in resonant raman systems for high-speed applications *OSA Annual Meeting (Rochester, NY, USA)* (Washington, DC: Optical Society of America)
[77] Uskov A V and Chang-Hasnain C 2005 Slow and superluminal light in semiconductor optical amplifiers *Electron. Lett.* **41** 922–4
[78] Harris S E 1997 Electromagnetically induced transparency *Phys. Today* **50** 36–42
[79] Adachi T, Ohno Y, Matsukura F and Ohno H 2001 Spin relaxation in n-modulation doped GaAs/AlGaAs (1 1 0) quantum wells *Phys. E: Low-Dimens. Syst. Nanostruct.* **10** 36–9
[80] Phillips M and Wang H 2002 Spin coherence and electromagnetically induced transparency via exciton correlations *Phys. Rev. Lett.* **89** 186401
[81] Phillips M and Wang H 2003 Electromagnetically induced transparency due to intervalence band coherence in a GaAs quantum well *Opt. Lett.* **28** 831–3
[82] Borri P, Langbein W, Schneider S, Woggon U, Sellin R L, Ouyang D and Bimberg D 2001 Ultralong dephasing time in InGaAs quantum dots *Phys. Rev. Lett.* **87** 157401
[83] Borri P, Langbein W, MÃ¸rk J, Hvam J M, Heinrichsdorff F, Mao M H and Bimberg D 1999 Dephasing in InAs/GaAs quantum dots *Phys. Rev.* B **60** 7784
[84] Hillman L W, Boyd R W, Krasinski J and Stroud C R, Jr. 1983 Observation of a spectral hole due to population oscillations in a homogeneously broadened optical absorption line *Opt. Commun.* **45** 416–9
[85] Chang S-W and Chuang S L 2005 Slow light based on population oscillation in quantum dots with inhomogeneous broadening *Phys. Rev.* B **72** 235330
[86] Derickson D 1998 *Fiber Optics Test and Measurement* (Englewood Cliffs, NJ: Prentice Hall)
[87] Kobayashi S and Kimura T 1980 Injection locking characteristics of an AlGaAs semiconductor laser *IEEE J. Quantum Electron.* **QE-16** 915–7
[88] Nakajima H 1990 Demodulation of multi-gigaHertz frequency-modulated optical signals in an injection-locked distributed feedback laser oscillator *Electron. Lett.* **26** 1129–31
[89] Bordonalli A C, Walton C and Seeds A J 1996 High-performance homodyne optical injection phase-lock loop using wide-linewidth semiconductor lasers *IEEE Photon. Technol. Lett.* **8** 1217–9
[90] Chang C-H, Chrostowski L and Chang-Hasnain C J 2003 Injection Locking of VCSELs *IEEE J. Sel. Top. Quant. Electron.* **9** 1386–93
[91] Chrostowski L and Zhao X 2006 Microwave performance of optically injection-locked VCSELs *IEEE Trans. Microw. Theory Tech.* **54** 788–96